Blind Modulation Classification of Different Variants of QPSK and 8-PSK for Multiple-Antenna Systems with Transmission Impairments

Rahul Gupta, Sudhan Majhi
Department of Electrical Engineering
Indian Institute of Technology Patna, India
Email: {smajhi, rahul.pee15}@iitp.ac.in

Octavia A. Dobre
Department of Electrical and Computer Engineering
Memorial University, St. John's, Canada
Email: odobre@mun.ca

***Abstract*—This work proposes the blind modulation classification (MC) of different variants of quadrature phase-shift-keying (QPSK), i.e., π/4-QPSK, offset QPSK (OQPSK), and minimum-shift-keying (MSK), and 8-PSK. The problem of MC for multiple antenna systems is investigated over frequency-selective fading channels with transmission impairments, i.e., phase, timing, and frequency offsets, without having prior information about channel coefficients. The MC algorithm proposed in this paper employs the cyclostationarity and higher-order statistical properties of the received baseband signal for classification. The MC is performed in three stages: at the first stage, the second-order cyclic cumulant uses the position of the cycle frequency to classify MSK and OQPSK. At the second and third stages, the fourth-order correlation function of the signals received from different antennas exhibits peaks, which are employed as discriminating features for QPSK, π/4-QPSK, and 8-PSK. Monte Carlo simulations are used to evaluate the performance of the proposed algorithm.**

***Index Terms*—Cyclostationarity, cyclic cumulant, correlation function, modulation classification.**

I. INTRODUCTION

BLIND modulation classification (MC) is a very important process of intelligent receivers before the demodulation of a signal. It plays a significant role in military, signal intelligence, electronics surveillance, emitter interception, where electronic warfare and threat analysis require the automatic classification of the received signal modulation, in order to locate, identify and jam hostile signals. It has also found a wide adoption in civilian applications [1]–[4], e.g., in the context of cognitive radio. Moreover, it is also important for network management, control and civilian applications. The MC for single antenna (single-input single-output (SISO)) systems has been predominantly investigated in [5]–[14].

A few works have been explored for multiple antenna systems [15]–[22]. The MC algorithms based on machine learning, cumulants, expectation-maximization, higher-order statistics, and cyclic cumulants (CCs) are discussed in [16]–[22]. The MC algorithms presented in [19] and [20] are restricted to the case when the number of transmit antennas is lower or equal to the number of receive antennas. The methods proposed in [21] and [22] are applicable to any number of receive and transmit antennas, without prior information about the channel coefficients. However, the features employed by these methods are the same for different variants of the quadrature phase-shift-keying (QPSK), i.e., offset QPSK (OQPSK), minimum-shift-keying (MSK), and π/4-QPSK. Accordingly, it is not possible to differentiate these modulation formats by using the existing algorithms. To the best of our knowledge, there exists no MC algorithm in the literature which applies to QPSK, OQPSK, π/4-QPSK, MSK, and 8-PSK modulations formats for multiple antenna systems. Moreover, π/4-QPSK is a variant of 8-PSK, and classifying them is another major problem under transmission impairments, i.e., phase, timing, and frequency offsets, and without the knowledge of the frequency-selective channel coefficients.

To address the above problems, we propose a new feature-based MC algorithm using the statistical properties of the CC and fourth-order correlation function. This is applicable to different types of wireless communication systems, including SISO, multiple-input multiple-output (MIMO), single-input multiple-output (SIMO), and multiple-input single-output (MISO) systems.

The paper is organized as follows. Section II introduces the signal model. Section III provides the analytical results for the second-order CC and fourth-order correlation used with the proposed MC algorithm. Section IV presents simulation results, and conclusions are drawn in Section V.

II. SIGNAL MODEL

We consider a MIMO system with N_t transmit and N_r receive antennas. The received baseband signal at the mth receive antenna is described as

$$y_m[n] = e^{j(2\pi f_0 n+\phi)} \sum_{q=0}^{N_t-1} \sum_{l=0}^{L-1} h_{qm}[l] x_q[n-l-\tilde{N}_1] + w_m[n], \quad (1)$$

where f_0 is the frequency offset normalized to the symbol rate, ϕ is the phase offset, $h_{qm}[l]$ is the fading channel coefficient between the qth transmit and mth receive antennas, $l = 0, ..., L-1$, with L as the maximum number of channel taps, $\tilde{N}_1$ is the number of timing offset samples, and $w_m[n]$ is the additive white Gaussian noise (AWGN) at the mth receive

978-1-5386-6358-5/18/$31.00 ©2018 IEEE

antenna. $x_q[n]$ is the transmitted signal from the qth transmit antenna, which can be written as $x_q[n] = x_{q_r}[n] + jx_{q_i}[n]$, where the I and Q components of $x_q[n]$ are given as $x_{q_r}[n]=\sum_{k=0}^{K-1} a_{q_r}[k]g[n-kP]$, $x_{q_i}[n]=\sum_{k=0}^{K-1} a_{q_i}[k]g[n-kP-\tilde{N}_2]$, with K as the number of symbols and $a_q[k]=a_{q_r}[k]+ja_{q_i}[k]$ as the kth symbol modulation format transmitted from the qth antenna. For $\{\text{QPSK, OQPSK, MSK}\}: a_{q_r}[k], a_{q_i}[k] = \pm 0.7071$, with $\tilde{N}_2 = P/2$ for OQPSK and MSK, and zero otherwise. Further, MSK is a special case of OQPSK with sinusoidal pulse weighting as given in Section III-A1, and for $\{\pi/4-\text{QPSK}, 8-\text{PSK}\}: a_{q_r}[k], a_{q_i}[k] = \pm 1, \pm 0.7071$. A root raised cosine (RRC) pulse $g[n]$ with roll-off factor β is used for spectral shaping, P is the oversampling factor ($P = F_s/f_s = T/T_s = N/K$), where F_s is the sampling rate, $f_s = 1/T$ is the symbol rate, T is the symbol period, $T_s = 1/F_s$ is the sampling period, and N is the received signal length.

III. Proposed Blind Modulation Classification Algorithm

A. First-Level Classification

At the first level, the cyclostationarity property of the second-order CC [23] is used to classify QPSK, OQPSK, π/4-QPSK, MSK, and 8-PSK. The mathematical derivation of the second-order CC for different modulation formats is described below.

1) Second-order CC for MSK modulated signal: The I and Q components of the transmitted MSK signal at the qth transmit antenna can be expressed as

$$x_{q_r}[n] = \sum_{k=0}^{K-1} a_{q_r}[k]g[n-kP]\cos(\pi n/P), \tag{2a}$$

$$x_{q_i}[n] = \sum_{k=0}^{K-1} a_{q_i}[k]g[n-kP-P/2]\sin(\pi n/P). \tag{2b}$$

Now, the second-order time-varying correlation function of the received complex baseband signal with zero time-lag is defined as

$$c_{y_m}[n;0] = \mathrm{E}\big[y_m[n]y_m^*[n]\big], \tag{3}$$

which for the I component can be expressed as

$$\begin{aligned} c_{y_{m_r}}[n;0] &= \sum_{q=0}^{N_t-1}\sum_{l=0}^{L-1} \big|h_{qm}[l]\big|^2 \sum_{k=0}^{K-1}\sum_{k'=0}^{K-1} \mathrm{E}\big[a_{q_r}(k)a_{q_r}^*(k')\big] \\ &\quad \times g[n-l-kP-\tilde{N}_1]g[n-l-k'P-\tilde{N}_1] \\ &\quad \times \cos^2[\pi n/P] + \sigma^2_{w_{m_r}}, \\ &= \frac{\sigma^2_{a_{q_r}}}{4P}\sum_{q=0}^{N_t-1}\sum_{l=0}^{L-1}\big|h_{qm}[l]\big|^2 \sum_{k=0}^{K-1} G[k/P]\, e^{j2\pi nk/P} \\ &\quad \times e^{-j2\pi k(\tilde{N}_1+l)/P}\big(e^{j2\pi n/P} + e^{-j2\pi n/P} + 2\big) \\ &\quad + \sigma^2_{w_{m_r}}, \end{aligned} \tag{4}$$

where $\sigma^2_{a_{q_r}} = \mathrm{E}\big[|a_{q_r}[k]|^2\big]$, $\sigma^2_{w_{m_r}} = \mathrm{E}\big[|w_{m_r}[n]|^2\big]$, and $G[\cdot]$ is the discrete Fourier transform (DFT) of $g^2[\cdot]$. Note that the final expression of (4) is obtained by using the Poisson sum formula [3]. The Fourier series coefficient of (4), $C_{y_{m_r}}[\alpha;0] = \lim_{N\to\infty} 1/N \sum_{n=0}^{N-1} c_{y_{m_r}}[n;0]e^{-j2\pi\alpha n}$, represents the CC at zero time-lag and cycle frequency α if it satisfies $C_{y_{m_r}}[\alpha;0] \neq 0$. The consistent estimator of $C_{y_{m_r}}[\alpha;0]$ is obtained as

$$\begin{aligned} \tilde{C}_{y_{m_r}}[\alpha;0] &\triangleq \frac{1}{N}\sum_{n=0}^{N-1} c_{y_{m_r}}[n;0]e^{-j2\pi\alpha n}, \\ &= \frac{\sigma^2_{a_{q_r}}}{4P}\sum_{q=0}^{N_t-1}\sum_{l=0}^{L-1}\big|h_{qm}[l]\big|^2 \sum_{k=0}^{K-1} G[k/P] \\ &\quad \times e^{-j2\pi k(\tilde{N}_1+l)/P}\big(2\delta[\alpha-k/P] \\ &\quad + \delta[\alpha-k/P-1/P] + \delta[\alpha-k/P+1/P]\big) \\ &\quad + \sigma^2_{w_{m_r}}\delta[\alpha]. \end{aligned} \tag{5}$$

Because the length of the received signal is limited, $\tilde{C}_{y_{m_r}}[\alpha;0]$ is seldom exactly zero even if α is not a cycle frequency, as shown in Fig. 1.

Similarly, for the Q component of the received signal, $y_{m_i}[n]$, the estimator of the CC $C_{y_{m_i}}[\alpha;0]$ at zero time-lag and cycle frequency α can be obtained as

$$\begin{aligned} \tilde{C}_{y_{m_i}}[\alpha;0] &= \frac{\sigma^2_{a_{q_i}}}{4P}\sum_{q=0}^{N_t-1}\sum_{l=0}^{L-1}\big|h_{qm}[l]\big|^2 \sum_{k=0}^{K-1} G[k/P] \\ &\quad \times e^{-j2\pi k(\tilde{N}_1+l)/P}\, e^{-j\pi k}\, \big(2\delta[\alpha-k/P] \\ &\quad - \delta[\alpha-k/P-1/P] - \delta[\alpha-k/P+1/P]\big) \\ &\quad + \sigma^2_{w_{m_i}}\delta[\alpha], \end{aligned} \tag{6}$$

where $\sigma^2_{a_{q_i}} = \mathrm{E}\big[|a_{q_i}[k]|^2\big]$ and $\sigma^2_{w_{m_i}} = \mathrm{E}\big[|w_{m_i}[n]|^2\big]$. Since a bandlimited filter is used, the CC $C_{y_m}[\alpha;0] = 0$ for $k > 1$ [3]. Thus, the estimator of the CC $C_{y_m}[\alpha;0]$ is obtained for $k = 0, 1$ as

$$\begin{aligned} \tilde{C}_{y_m}[\alpha;0] &= \frac{1}{4P}\sum_{q=0}^{N_t-1}\sum_{l=0}^{L-1}\big|h_{qm}[l]\big|^2 \Big\{ 2\delta[\alpha]\big(\sigma^2_{a_{q_r}} + \sigma^2_{a_{q_i}}\big) \\ &\quad + \big(\delta[\alpha-1/P] + \delta[\alpha+1/P]\big)\big(\sigma^2_{a_{q_r}} - \sigma^2_{a_{q_i}}\big) \\ &\quad + G[1/P]\, e^{-j2\pi(\tilde{N}_1+l)/P}\Big(2\delta[\alpha-1/P]\big(\sigma^2_{a_{q_r}} \\ &\quad - \sigma^2_{a_{q_i}}\big) + \big(\delta[\alpha-2/P] + \delta[\alpha]\big)\big(\sigma^2_{a_{q_r}} + \sigma^2_{a_{q_i}}\big)\Big)\Big\} \\ &\quad + \sigma^2_{w_m}\delta[\alpha], \end{aligned} \tag{7}$$

where $\sigma^2_{w_m} = \sigma^2_{w_{m_r}} + \sigma^2_{w_{m_i}}$. As the power of the I and Q components of $a_q[m]$ is the same, $\sigma^2_{a_{q_r}} - \sigma^2_{a_{q_i}} = 0$, and the final expression is

$$\begin{aligned} \tilde{C}_{y_m}[\alpha;0] &= \frac{1}{4P}\sum_{q=0}^{N_t-1}\sum_{l=0}^{L-1}\big|h_{qm}[l]\big|^2\big(\sigma^2_{a_{q_r}} + \sigma^2_{a_{q_i}}\big)\Big\{2\delta[\alpha] + G[1/P] \\ &\quad \times e^{-j2\pi(\tilde{N}_1+l)/P}\big(\delta[\alpha-2/P] + \delta[\alpha]\big)\Big\} + \sigma^2_{w_m}\delta[\alpha]. \end{aligned} \tag{8}$$

2) Second-order CC for QPSK, π/4-QPSK, OQPSK, and 8-PSK modulated signals: First, for classifying QPSK, π/4-QPSK, and 8-PSK modulated signals, we derived the estimator of $C_{y_m}[\alpha;0]$, similar to the above analysis at zero time-lag and cycle frequency α for $k=0,1$ as

$$\tilde{C}_{y_m}[\alpha;0]=\frac{1}{P}\sum_{q=0}^{N_t-1}\sum_{l=0}^{L-1}\left|h_{qm}[l]\right|^2\left(\sigma^2_{a_{q_r}}+\sigma^2_{a_{q_i}}\right)\Big\{\delta[\alpha] + G\left[1/P\right]e^{-j2\pi(\tilde{N}_1+l)/P}\delta[\alpha-1/P]\Big\}+\delta[\alpha]\sigma^2_{w_m}. \tag{9}$$

For the OQPSK modulated signal, $\tilde{N}_2{=}P/2$, and hence, we get the extra term $e^{-j\pi k}$ in the Q component of the received signal. Finally, the estimator of the CC for OQPSK modulated signal for $k=0,1$ is obtained as

$$\tilde{C}_{y_m}[\alpha;0]=\frac{1}{P}\sum_{q=0}^{N_t-1}\sum_{l=0}^{L-1}\left|h_{qm}[l]\right|^2\Big\{\delta[\alpha]\left(\sigma^2_{a_{q_r}}+\sigma^2_{a_{q_i}}\right)+G\left[1/P\right] \times e^{-j2\pi(\tilde{N}_1+l)/P}\delta[\alpha-1/P]\left(\sigma^2_{a_{q_r}}-\sigma^2_{a_{q_i}}\right)\Big\} + \delta[\alpha]\sigma^2_{w_m}. \tag{10}$$

In (10), as the power of the I and Q components of $a_q[m]$ is the same, $\sigma^2_{a_{q_r}}-\sigma^2_{a_{q_i}}=0$, and the final expression is

$$\tilde{C}_{y_m}[\alpha;0]=\frac{1}{P}\sum_{q=0}^{N_t-1}\sum_{l=0}^{L-1}\left|h_{qm}[l]\right|^2\delta[\alpha]\left(\sigma^2_{a_{q_r}}+\sigma^2_{a_{q_i}}\right)+\delta[\alpha]\sigma^2_{w_m}. \tag{11}$$

In practice, the CC estimate at zero time-lag and cycle frequency α is simply calculated as [23]

$$\tilde{C}_{y_m}[\alpha;0]\triangleq\frac{1}{N}\sum_{n=0}^{N-1}\left|y_m[n]\right|^2 e^{-j2\pi n\alpha}. \tag{12}$$

Equation (12) is the normalized DFT of $|y_m[n]|^2$, and can simply be implemented by the fast Fourier transform algorithm. Once $\tilde{C}_{y_m}[\alpha;0]$ is obtained, the frequency estimation is straightforward [23]

$$\hat{f}_m=\arg\max_{\alpha\in[u,v]}\left|\tilde{C}_{y_m}[\alpha;0]\right|, \tag{13}$$

where $[u,v]$ is the lower and upper bound search interval, $u{=}\alpha_u N/F_s$ and $v{=}\alpha_v N/F_s$, $[\alpha_u,\alpha_v]\equiv[f_{bw}/2, f_{bw}/1.2]$; this interval is obtained through extensive simulation studies, with f_{bw} as the 3 dB signal bandwidth. As we deal with multiple antenna systems having N_r received antennas, we have $\hat{f}_m$ for $m=0,...,N_r-1$ estimated frequencies. If any of the links are effected by deep fade, the other links provide the features for the classification of the modulation formats.

From (8), a second-order CC peak for MSK modulated signal appears at $\alpha=2/P$, i.e., at $2f_s$ as shown in Fig. 1. From (9), QPSK, π/4-QPSK, and 8-PSK modulated signals exhibit a peak at $\alpha=1/P$, i.e., at f_s and for OQPSK as in (11) there is no peak, as shown in Fig. 1. Since QPSK, π/4-QPSK, and 8-PSK do not have distinct features for the second-order CC, we further investigate their distinct features for the second-level classification stage.

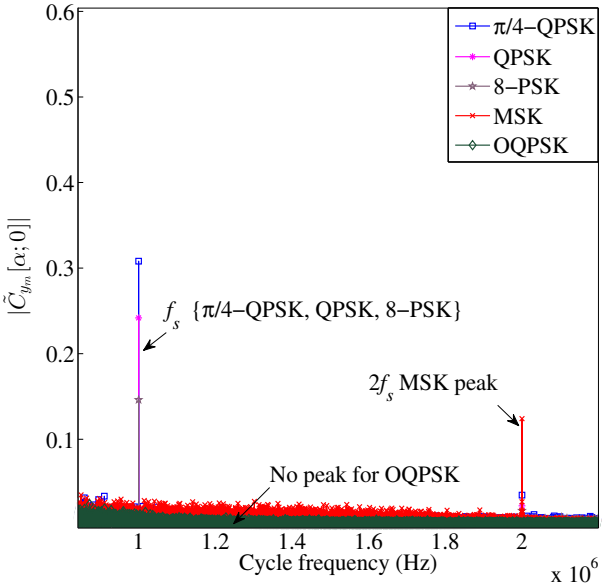

Fig. 1. Estimate of the second-order CC peaks for QPSK, π/4-QPSK, OQPSK, MSK, and 8-PSK modulated signals at $f_s=1$ MHz.

B. Second-Level Classification

At this level, the fourth-order correlation function is used as a distinct feature for the classification of the modulation formats. This is defined as [21]

$$B_{m,m'}(p)=\mathrm{E}\left[\left(y_m[n]\right)^2\left(y_{m'}[n+p]\right)^2\right], \tag{14}$$

where $m,m'=0,1,...,N_r-1$, $m\neq m'$. From (14), it is found that QPSK exhibits peaks, while π/4-QPSK and 8-PSK do not, as shown in Fig. 2 for $K{=}10000$ and $P{=}10$.

C. Third-Level Classification

At the final level, we have two modulation formats π/4-QPSK and 8-PSK, which need to be classified. First, we split the received baseband signal into odd $y^o_m[\hat{n}]$ and even $y^e_m[\tilde{n}]$ symbols as

$$y^o_m[n]=y_m[Pr+i_1],\ r=0,2,...,N, \tag{15a}$$
$$y^e_m[n]=y_m[Ps+i_1],\ s=1,3,...,N-1, \tag{15b}$$

where $0\leq i_1<P$. Now, the fourth-order correlations of these symbols are given as

$$B^o_{m,m'}(p)=\mathrm{E}\left[\left(y^o_m[n]\right)^2\left(y^o_{m'}[n+p]\right)^2\right], \tag{16a}$$
$$B^e_{m,m'}(p)=\mathrm{E}\left[\left(y^e_m[n]\right)^2\left(y^e_{m'}[n+p]\right)^2\right]. \tag{16b}$$

For the π/4-QPSK, separated even and odd symbols exhibit QPSK constellations rotated by π/4 with respect to each other. As such, (16a) and (16b) provide peaks for π/4-QPSK, while there are no peaks for 8-PSK, as shown in Fig. 3.

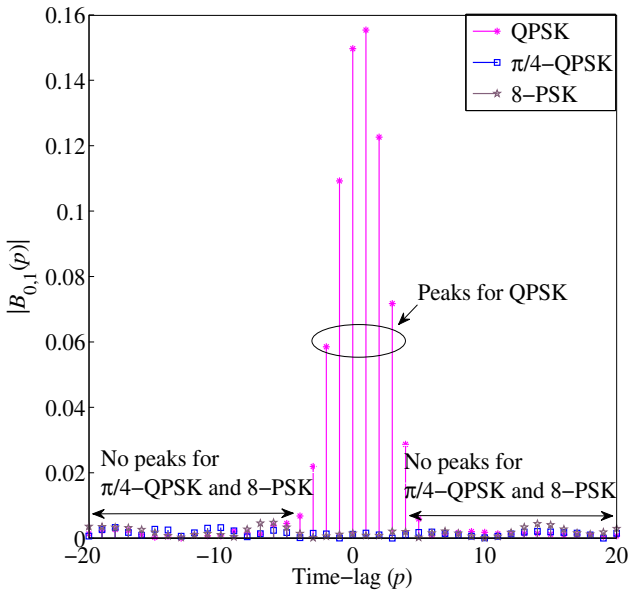

Fig. 2. The magnitude of the fourth-order correlation function, K=10000, L=4, and P=10 for QPSK, π/4-QPSK, and 8-PSK modulated signals.

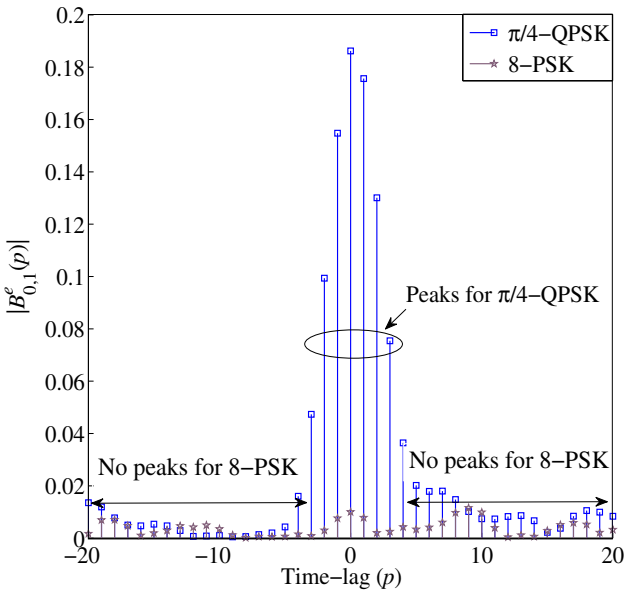

Fig. 3. The magnitude of the fourth-order correlation function, K=20000, L=4, and P=10 for π/4-QPSK and 8-PSK modulated signals.

IV. Simulation Results and Discussion

The performance of the proposed MC algorithm was evaluated using Monte Carlo simulations. The performance is measured for 10000 trials and the number of symbols for each trial is set to 20000. We considered a pool of modulations: QPSK, π/4-QPSK, OQPSK, MSK, 8-PSK. Frequency-selective Rayleigh fading channel is considered with $L=4$ and 8 channel taps, respectively, and 0.5 roll-off factor is used with the RRC pulse shape filter. The receiver sampling rate is 50 MHz, which results in an oversampling factor of $P = 10$ ($P = F_s/f_s = 50$ MHz/5 MHz $= 10$), while the symbol rate is varied between 1 MHz and 5 MHz. The signal-to-noise ratio (SNR) is defined as SNR $= N_t\sigma_s^2/\sigma_n^2$, with σ_s^2 and σ_n^2 as the transmit power per antenna and the variance of the AWGN, respectively. The phase and timing offset are introduced randomly by the channel; we introduce these in simulation as $\phi \in [-\pi, \pi)$ and $\tilde{N}_1 \in [-100, 100]$. Moreover, if a frequency offset error about $\pm 100 - \pm 1000$ Hz is present in the received baseband signals, it does not affect the classification performance.

Fig. 4 shows the percentage of correct classification (P_{cc}) for all five modulation formats, i.e., QPSK, π/4-QPSK, OQPSK, MSK, 8-PSK, achieved with the proposed algorithm. Simulation results are shown for different types of wireless communication systems, including SISO, MIMO, SIMO, and MISO systems in the presence of phase, timing, and frequency offsets over frequency-selective fading channels. By comparing results in Fig. 4, it is noted that improved results are attained for $N_r = 2$ when compared with $N_r = 1$ as expected. It is also observed that the performance of the proposed classification algorithm is independent of the number of channel taps. This shows its advantage, i.e., it does not require knowledge of the channel coefficients.

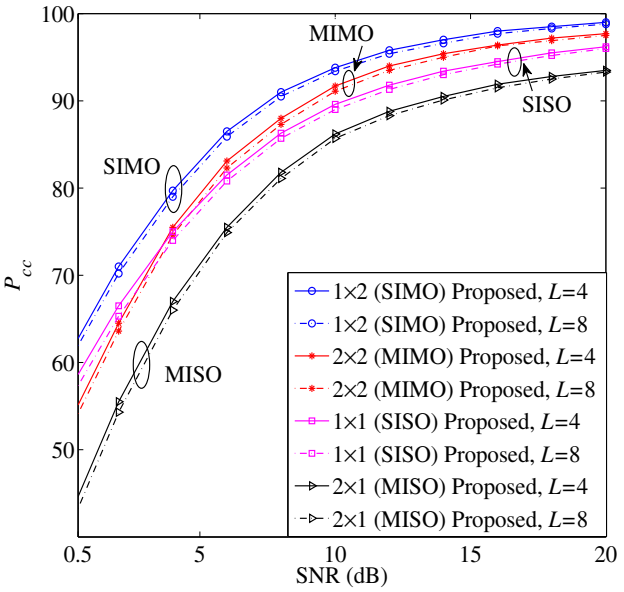

Fig. 4. P_{cc} vs. SNR for {QPSK, π/4-QPSK, OQPSK, 8-PSK, and MSK} modulation formats, with different antenna configurations ($N_t = 1, 2$, $N_r = 1, 2$) for $L = 4, 8$.

Fig. 5 presents the performance comparison of the proposed MC algorithm with existing works, for the QPSK and 8-PSK modulation formats. It is noticed that the proposed algorithm outperforms the algorithm discussed in [8] and [9] for SISO system. It is also observed that the proposed MC algorithm

and the method in [21] have a similar performance for SISO and SIMO. However, the method in [21] can be applied only to the classification of QPSK and 8-PSK modulations, whereas the proposed algorithm is suitable to a larger pool of QPSK modulations and also works for the MIMO and MISO systems with better classification performance. The computational complexity of the proposed algorithm is of $\mathcal{O}(Nlog_2N)$. The computational complexity of cumulant, correlation function, and maximum likelihood algorithm is of $\mathcal{O}(N)$, $\mathcal{O}(N)$, and $\mathcal{O}(N \times M_a \times I)$ respectively, where N is the received signal length, M_a is the constellation size of the ath modulation scheme and I is the total number of modulation schemes used for classification.

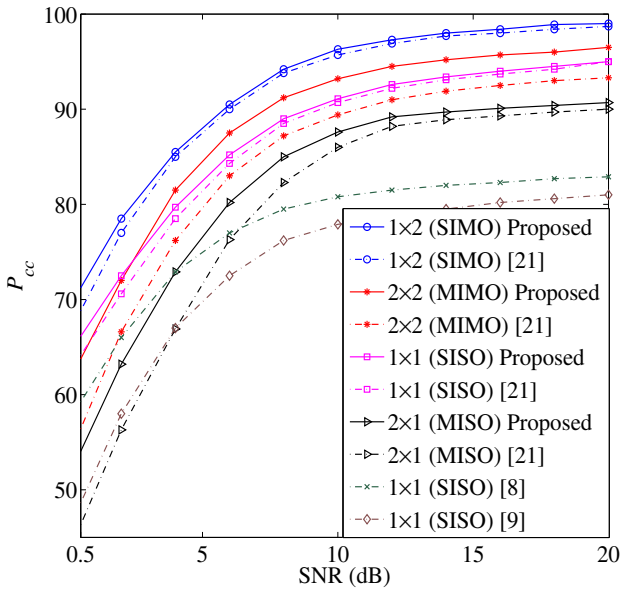

Fig. 5. Comparison of P_{cc} vs. SNR for {QPSK and 8-PSK} for MIMO, SIMO, MISO, and SISO systems.

V. Conclusion

Analysis and simulation results show that the second-order CC and fourth-order correlation of the received baseband signal exhibit peaks for different modulation formats. Unlike previously reported MC algorithms, a new algorithm has been proposed for SISO, SIMO, MISO, and MIMO systems, which can classify different variant of QPSK modulation formats, i.e., QPSK, π/4-QPSK, OQPSK, and MSK, and 8-PSK, transmitted over frequency-selective fading channels. This also works in the presence of timing, phase, and frequency offsets, without having prior information about the channel. Simulation results show that the proposed MC algorithm can achieve a satisfactory classification performance as compared to existing methods.

References

[1] O. A. Dobre, A. Abdi, Y. Bar-Ness, and W. Su, "Survey of automatic modulation classification techniques: Classical approaches and new trends," *IET Commun.*, vol. 1, no. 2, pp. 137 –156, Apr. 2007.

[2] S. Majhi, M. Kumar, and W. Xiang, "Implementation and measurement of blind wireless receiver for single carrier systems," *IEEE Trans. Instrum. and Meas.*, vol. 66, no. 8, pp. 1965–1975, Aug. 2017.

[3] S. Majhi and T. S. Ho, "Blind symbol-rate estimation and testbed implementation of linearly modulated signals," *IEEE Trans. Veh. Technol.*, vol. 64, no. 3, pp. 954–963, Sep. 2015.

[4] Y. A. Eldemerdash, O. A. Dobre, O. Ureten, and T. Yensen, "Identification of cellular networks for intelligent radio measurements," *IEEE Trans. Instrum. and Meas.*, vol. 66, no. 8, pp. 2204–2211, Aug. 2017.

[5] W. Wei and J. M. Mendel, "Maximum-likelihood classification for digital amplitude-phase modulations," *IEEE Trans. Commun.*, vol. 48, no. 2, pp. 189–193, Feb. 2000.

[6] S. Majhi, R. Gupta, W. Xiang, and S. Glisic, "Hierarchical hypothesis and feature-based blind modulation classification for linearly modulated signals," *IEEE Trans. Veh. Technol.*, vol. PP, no. 99, pp. 1–1, Jul. 2017.

[7] A. Abdi, O. A. Dobre, R. Choudhry, Y. Bar-Ness, and W. Su, "Modulation classification in fading channels using antenna arrays," in *Proc. 2004 IEEE Military Communication Conference*, pp. 211–217.

[8] H.-C. Wu, M. Saquib, and Z. Yun, "Novel automatic modulation classification using cumulant features for communications via multipath channels," *IEEE Trans. Wireless Commun.*, vol. 7, no. 8, pp. 3098 –3105, Aug. 2008.

[9] V. D. Orlic and M. L. Dukic, "Automatic modulation classification algorithm using higher-order cumulants under real-world channel conditions," *IEEE Commun. Lett.*, vol. 13, no. 12, pp. 917–919, Dec. 2009.

[10] S. Majhi, R. Gupta, and W. Xiang, "Novel blind modulation classification of circular and linearly modulated signals using cyclic cumulants," in *Proc. 2017 IEEE International Symposium on Personal, Indoor, and Mobile Radio Communications*, pp. 1–5.

[11] O. A. Dobre, M. Oner, S. Rajan, and R. Inkol, "Cyclostationarity-based robust algorithms for QAM signal identification," *IEEE Commun. Lett.*, vol. 16, no. 1, pp. 12–15, Jan. 2012.

[12] M. Oner and O. A. Dobre, "On the second-order cyclic statistics of signals in the presence of receiver impairments," *IEEE Trans. Commun.*, vol. 59, no. 12, pp. 3278–3284, Dec. 2011.

[13] W. A. Jerjawi, Y. A. Eldemerdash, and O. A. Dobre, "Second-order cyclostationarity-based detection of LTE SC-FDMA signals for cognitive radio systems," *IEEE Trans. Instrum. and Meas.*, vol. 64, no. 3, pp. 823–833, Mar. 2015.

[14] O. A. Dobre, Y. Bar-Ness, and W. Su, "Higher-order cyclic cumulants for high order modulation classification," in *Proc. 2003 IEEE Military Communication Conference*, pp. 112 – 117.

[15] Y. A. Eldemerdash, O. A. Dobre, and M. Oner, "Signal identification for multiple-antenna wireless systems: Achievements and challenges," *IEEE Commun. Surv. Tutor.*, vol. 18, no. 3, pp. 1524–1551, third quarter 2016.

[16] X. Liu, C. Zhao, P. Wang, Y. Zhang, and T. Yang, "Blind modulation classification algorithm based on machine learning for spatially correlated MIMO system," *IET Commun.*, vol. 11, no. 7, pp. 1000–1007, Dec. 2017.

[17] M. S. Mhlhaus, M. Oner, O. A. Dobre, H. U. Jkel, and F. K. Jondral, "Automatic modulation classification for MIMO systems using fourth-order cumulants," in *Proc. 2012 IEEE Vehicular Technology Conference (VTC Fall)*, pp. 1–5.

[18] Z. Zhu and A. K. Nandi, "Blind modulation classification for MIMO systems using expectation maximization," in *Proc. 2014 IEEE Military Communication Conference*, pp. 754–759.

[19] K. Hassan, I. Dayoub, W. Hamouda, C. N. Nzeza, and M. Berbineau, "Blind digital modulation identification for spatially-correlated MIMO systems," *IEEE Trans. Wireless Commun.*, vol. 11, no. 2, pp. 683–693, Feb. 2012.

[20] M. S. Muhlhaus, M. Oner, O. A. Dobre, and F. K. Jondral, "A low complexity modulation classification algorithm for MIMO systems," *IEEE Commun. Lett.*, vol. 17, no. 10, pp. 1881–1884, Oct. 2013.

[21] M. Marey and O. A. Dobre, "Blind modulation classification algorithm for single and multiple-antenna systems over frequency-selective channels," *IEEE Signal Process. Lett.*, vol. 21, no. 9, pp. 1098–1102, Sep. 2014.

[22] ——, "Blind modulation classification for alamouti STBC system with transmission impairments," *IEEE Wireless Commun. Lett.*, vol. 4, no. 5, pp. 521–524, Oct. 2015.

[23] G. Giannakis and G. Zhou, "Harmonics in multiplicative and additive noise: Parameter estimation using cyclic statistics," *IEEE Trans. Signal Process.*, vol. 43, no. 9, pp. 2217 –2221, Sep. 1995.